# Characterizing short disperision-length fiber via dispersive virtual reference interferometry

**Michael A. Galle,[1,*] Eric Y. Zhu,[1] Simarjeet S. Saini,[2] Waleed S. Mohammed,[3] and Li Qian[1]**

[1]*Dept.of Elec. and Computer Engineering, Univ. of Toronto, 10 King's College Road, Toronto, Ontario, Canada*
[2]*Dept.of Elec. and Computer Engineering, Univ. of Waterloo, 200, University Avenue W., Waterloo, Ontario, Canada*
[3]*Center of Optoelectronics, Communication and Control Systems (BU-CROCCS), School of Engineering, Bangkok University, Pahunyouthin Road, Phatumthani, 12120, Thailand*
[*]*michael.galle@utoronto.ca*

**Abstract:** The ability to characterize fibers with near-zero dispersion-length products is of considerable practical interest. We introduce dispersive virtual reference interferometry (DVRI) as a technique for the characterization of short length (<1m) fibers with near-zero disperison-length. DVRI has an accuracy equivalent to standard balanced spectral interferometry (on the order of $10^{-3}$ ps and $10^{-5}$ ps/nm for the group delay and dispersion-length measurements respectively) but does not require wide spectral bandwidths or multiple spectral scans. Following experimental validation, the DVRI technique is used to characterize a 23.3-cm erbium-doped gain fiber (dispersion-length product <0.002 ps/nm), using a tunable laser with a bandwidth of 145nm. Furthermore, the dispersion in a 28.6-cm commercial dispersion shifted fiber is characterized across the zero-dispersion wavelength and the zero-disperison-wavelength and slope were determined to be 1566.7 nm and $8.57 \times 10^{-5}$ ps/(nm$^2$·m) with a precision of ± 0.2 nm and ± $0.06 \times 10^{-5}$ ps/(nm$^2$·m), respectively.



**OCIS codes:** (060.2270) Fiber characterization; (060.2410) Fibers, erbium; (120.3180) Interferometry; (120.3930) Metrological instrumentation; (120.3688) Lightwave analyzers.

## References and links

1. L. G. Cohen, "Comparison of single-mode fiber dispersion measurement techniques," J. Lightwave Technol. **3**(5), 958–966 (1985).
2. C. Palavicini, Y. Jaouën, G. Debarge, E. Kerrinckx, Y. Quiquempois, M. Douay, C. Lepers, A. F. Obaton, and G. Melin, "Phase-sensitive optical low-coherence reflectometry technique applied to the characterization of photonic crystal fiber properties," Opt. Lett. **30**(4), 361–363 (2005).
3. F. Sears, L. Cohen, and J. Stone, "Interferometric measurements of dispersion-spectra variations in a single-mode fiber," J. Lightwave Technol. **2**(2), 181–184 (1984).
4. P. A. Merritt, R. P. Tatam, and D. A. Jackson, "Interferometric chromatic dispersion measurements on short lengths of monomode optical fiber," J. Lightwave Technol. **7**(4), 703–716 (1989).
5. R. Cella and W. Wood, "Measurement of Chromatic Dispersion in Erbium-Doped Fiber using Low Coherence Interferometry," in *Proceedings of the Sixth Optical Fibre Measurement Conference* (2001), pp. 207–210.
6. P. Lu, H. Ding, and S. J. Mihailov, "Direct measurement of the zero-dispersion wavelength of tapered fibres using broadband-light interferometry," Meas. Sci. Technol. **16**(8), 1631–1636 (2005).
7. J. Y. Lee and D. Y. Kim, "Versatile chromatic dispersion measurement of a single mode fiber using spectral white light interferometry," Opt. Express **14**(24), 11608–11615 (2006).
8. W. Mohammed, J. Meier, M. A. Galle, L. Qian, J. S. Aitchison, and P. W. E. Smith, "Linear and quadratic dispersion characterization of millimeter-length fibers and waveguides using common-path interferometry," Opt. Lett. **32**(22), 3312–3314 (2007).
9. M. A. Galle, S. S. Saini, W. S. Mohammed, and L. Qian, "Virtual reference interferometry: theory and experiment," J. Opt. Soc. Am. B **29**(11), 3201–3210 (2012).
10. Corning® Inc., "Corning® SMF-28™ Product Information," http://ece466.groups.et.byu.net/notes/smf28.pdf.

#210066 - $15.00 USD Received 14 Apr 2014; revised 23 May 2014; accepted 29 May 2014; published 3 Jun 2014

## 1. Introduction

Chromatic dispersion is an important parameter for a host of specialty fibers, such as photonic crystal fibers, gain fibers, and dispersion-engineered fibers. Because of cost and other practical considerations, dispersion characterization on short lengths of fiber is highly desirable. For example, doped gain fibers have high absorption near the gain region when they are not pumped, limiting the length of the fiber that can be used for dispersion characterization. When length is constrained, so is the total dispersion-length product (*DL*), defined as the second-order dispersion parameter (*D*) multiplied by the length of the fiber (*L*). The *DL* product is the cumulative group delay difference per unit bandwidth over the entire fiber length. Commercial dispersion characterization instruments, based on time-of-flight or modulation phase-shift, typically have a time resolution of 20-100 ps/nm [1]. As a result they require long fiber lengths to make an accurate characterization, particularly when the fiber dispersion is low. For the characterization of short fiber lengths (<1m), however, Interferometric techniques are commonly used [1]. These techniques may be classified into temporal [2, 3] and spectral [4–8] interferometry. Spectral interferometry may be further subdivided into balanced spectral interferometry (BSI) [4–6] and unbalanced spectral interferometry (USI) [7, 8]. Among these techniques, only BSI is capable of extracting second-order dispersion directly from the interference pattern, independent of the group delay measurement [4].

In BSI, the group delay in the test arm (containing the test fiber) is balanced by that in the reference arm. Balancing results in an inteferogram whose intensity variation contains information about the difference ( $\Delta$ ) in the second-order dispersion length (*DL*) between the test and reference arm. The minimum spectral bandwidth needed to characterize a fiber using BSI is inversely proportional to $\sqrt{\Delta}$ [6, 9]. Since the reference path in BSI is typically free space, which has zero second-order dispersion, the $\Delta$ measured from the interferogram using a free space path is simply the *DL* of the test fiber itself. As a result, the lower limit on the *DL* that can be measured is limited by the available bandwidth. Recently we introduced a technique called Virtual Reference Interferometry (VRI) [9] to eliminate the need for the free space reference arm in BSI. VRI produces a second-order interference pattern using a *simulated* reference path, from which the *DL* of the test fiber can be extracted directly, in a manner analogous to BSI [4, 9]. Like BSI, however, using a simulated free-space reference also puts a lower limit on the *DL* that can be measured. However, since the reference is simulated in VRI, the simulation parameters may include a dispersive reference path. Using a dispersive reference path (with high second-order dispersion) lowers the *DL* measurement limit (which is in principle, limited by the fringe resolution) without requiring an increase in the scan range (bandwidth). This is achieved because the dispersion difference between the test arm and the virtual reference arm can be artificially increased (i.e. by increasing the dispersion of the virtual reference), leading to a spectrally denser second-order interference fringe pattern. This allows the extraction of $\Delta$ over a smaller spectral region. For the same reason, this strategy also leads to an increase in the wavelength range over which the second-order dispersion of the fiber can be characterized. To distinguish from the VRI technique used in [9], we shall use the term dispersive-VRI or DVRI to indicate the use of a simulated dispersive reference in this manuscript. We will first derive theoretical relationships between the dispersion of the virtual reference, that of the test fiber, and the properties of the interferogram. The DVRI technique will then be used experimentally for the characterization of short-length, low-dispersion gain fibers and dispersion shifted fibers.

## 2. Theory

The detailed steps in a DVRI measurement are exactly as presented for VRI in [9], with the exception that a dispersive reference will now be used. A summary of the steps in a DVRI measurement are now presented. The first step in a DVRI measurement is to obtain a spectral

#210066 - $15.00 USD Received 14 Apr 2014; revised 23 May 2014; accepted 29 May 2014; published 3 Jun 2014

interference pattern by interfering the reflections from the two cleaved or polished facets of a test fiber. The intensity measured at the detector, after normalization of the amplitude, is given by Eq. (1) [9]

$$I_{\mathrm{Real}}(\lambda) \cong \cos(2\beta_f(\lambda)L_f) \tag{1}$$

where $\lambda$ is the wavelength, $\beta_f$ is the propagation constant of the test fiber and $L_f$ is its length. In the second step, a simulated interference pattern is generated numerically using a dispersive virtual reference path via Eq. (2)

$$I_{virtual}(\lambda,\lambda_0) = \cos(2\beta_v(\lambda)L_v) \tag{2}$$

where $\beta_v(\lambda)$ is the propagation constant of the dispersive virtual reference and $L_v$ is its length. Note here $L_v$ is chosen such that the group delay of the virtual reference balances that of the test fiber at a given wavelength $\lambda_o$, illustrated in Fig. 1. In the third step the simulated interference pattern in Eq. (2) is multiplied (point-by-point) with the real interference pattern in Eq. (1) to produce a second-order interference pattern described by Eq. (3)

$$I_{SO}(\lambda,\lambda_0) = \underbrace{\cos\left(2\left(\beta_f(\lambda)L_f - \beta_v(\lambda)L_v\right)\right)}_{\text{slow varying term}}\underbrace{\cos\left(2\left(\beta_f(\lambda)L_f + \beta_v(\lambda)L_v\right)\right)}_{\text{fast varying term}} \tag{3}$$

and illustrated in Fig. 1. Note that this interferogram has a fast-varying term, amplitude modulated by a slow-varying term. The modulation amplitude changes according to its phase as described by Eq. (4)

$$\varphi_{Amp.\mathrm{mod.}}(\lambda) = 2\left|\beta_f(\lambda)L_f - \beta_v(\lambda)L_v\right| = 2k_0\left|n_{eff_f}(\lambda)L_f - n_{eff_v}(\lambda)L_v\right| \tag{4}$$

where $k_0$ is the propagation constant in free space, $n_{eff_f}(\lambda)$ is the refractive index of the test fiber, and $n_{eff_v}(\lambda)$ is the simulated refractive index of the refence path. Note that the magnitude is taken since $\cos(-\varphi) = \cos(\varphi)$.

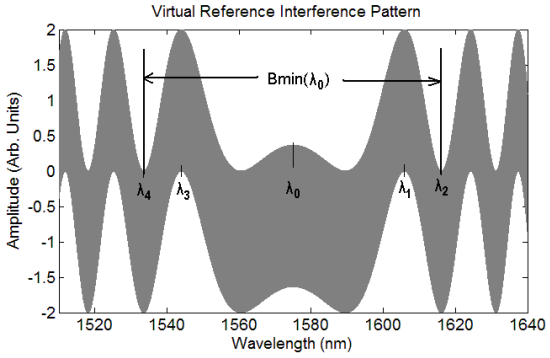


Fig. 1. Amplitude modulated interference pattern described by Eq. (3). The fast varying interference is shown in grey and is not resolved in the figure. The slow varying amplitude modulation with phase described by Eq. (4) is shown.

The amplitude modulation exhibits a symmetry at wavelength $\lambda_0$ (Fig. 1), where the group index × length of the fiber and that of the virtual reference are balanced as shown in Eq. (5)

$$N_{gv}(\lambda_0)L_v = N_{g_f}(\lambda_0)L_f \tag{5}$$

#210066 - $15.00 USD Received 14 Apr 2014; revised 23 May 2014; accepted 29 May 2014; published 3 Jun 2014

The value of $N_{gv}(\lambda_0)L_v$ (the group index × length of the virtual reference) that produces the symmetry point at a desirable wavelength allows us to obtain the first order dispersion $N_{gf}(\lambda_0)L_f$ (the group index × length of the fiber) at this wavelength for the test fiber. Note that in order to accurately locate the symmetry point, $\lambda_0$, a peak and valley must be visible on each side of $\lambda_0$ as illustrated in Fig. 1. Furthermore, at least one peak and one valley on each side of $\lambda_0$ must also be visible within the scan range in order to be able to measure second order dispersion directly from the interference pattern [6, 9]. As a result, the minimum bandwidth required ( $B_{\min}(\lambda_0)$ in Fig. 1) is given by the spectral separation between $\lambda_2$ and $\lambda_4$. Where, following the procedure in [6, 9], the relationship between the minimum bandwidth $B_{\min}(\lambda_0)$ can be related to the dispersion length difference between the test and reference paths $\Delta(\lambda_0)$ as in Eq. (6)

$$B_{\min}(\lambda_0) \cong \left(\frac{6\lambda_0}{\Delta(\lambda_0)}\right)^{\frac{1}{2}} \tag{6}$$

where increasing $\Delta(\lambda_0)$ reduces $B_{\min}(\lambda_0)$. Taylor expanding $n_{eff_f}(\lambda)$ and $n_{eff_v}(\lambda)$ in Eq. (4) and neglecting terms higher than third order gives the expression for the phase difference between two peak or valley points shown in Eq. (7).

$$\left|\underset{\text{mod.}}{\varphi_{Amp.}}(\lambda_m) - \underset{\text{mod.}}{\varphi_{Amp.}}(\lambda_n)\right| \cong 2\pi\left|\left[\frac{(\lambda_m-\lambda_0)^2}{\lambda_m} - \frac{(\lambda_n-\lambda_0)^2}{\lambda_n}\right]\Delta(\lambda_0) + \left[\frac{(\lambda_m-\lambda_0)^3}{3\lambda_m} - \frac{(\lambda_n-\lambda_0)^3}{3\lambda_n}\right]\left.\frac{d\Delta}{d\lambda}\right|_{\lambda_0}\right| \tag{7}$$
$$\cong \pi(m-n)$$

where $\Delta(\lambda_0) = d^2 n_{eff_f}/d\lambda^2\big|_{\lambda_0} L_f - d^2 n_{eff_v}/d\lambda^2\big|_{\lambda_0} L_v$, $d\Delta/d\lambda\big|_{\lambda_0}$ accounts for the effects of third order dispersion, and $(m-n)$ is the number of peak-to-valley or valley-to-peak transitions between a peak or valley at $\lambda_n$ and one at $\lambda_m$. Note that the points are chosen such that either $\lambda_m > \lambda_n > \lambda_0$ or $\lambda_m < \lambda_n < \lambda_o$. For example, in Fig. 1 $m = 2$ and $n = 1$ so that Eq. (7) gives the phase separation between $\lambda_2$ and $\lambda_1$ as $\pi$. The same result is obtained for $m = 4$ and $n = 3$. Using $D(\lambda_0) = -\frac{\lambda_0}{c} d^2 n_{eff}/d\lambda^2\big|_{\lambda_0}$, the $|\Delta(\lambda_0)|$ term in Eq. (7) can be expressed as Eq. (8)

$$|\Delta(\lambda_0)| \equiv \frac{c}{\lambda_0}\left|D_v(\lambda_0)L_v - D_f(\lambda_0)L_f\right| \tag{8}$$

An important result of Eq. (8) is that an arbitrarily large $D_v(\lambda_0)L_v$ may be simulated to make $|\Delta(\lambda_0)|$ large so that $B_{\min}(\lambda_0)$ in Eq. (6) is less than the source (scan) bandwidth. We refer to the reduction in $B_{\min}(\lambda_0)$ as *compression* of the interferogram. Note that since the sign of $\Delta(\lambda_0)$ is unknown, there are two possibilities for the value of $D_f(\lambda_0)L_f$. However, by comparing the second-order interferograms produced using both positive $D_v(\lambda_0)L_v$ and negative $D_v(\lambda_0)L_v$, one can easily remove this ambiguity.

The selection of the dispersion of the virtual arm is essential to enabling the measurement of fiber with near-zero dispersion-length. Hence, we now discuss how to determine the appropriate parameters for the dispersive virtual reference. Although there are many

#210066 - $15.00 USD Received 14 Apr 2014; revised 23 May 2014; accepted 29 May 2014; published 3 Jun 2014

possibilities for the design of the dispersive reference, the simplest design defines the group index × length as a first order polynomial as described by Eq. (9).

$$N_{gv}(\lambda)L_v = K(\lambda - a) + b \tag{9}$$

Where $K$, $a$ and $b$ are parameters of the dispersive virtual reference. $K$ is a unitless parameter, however, both $b$ and $a$ are expressed in meter units. The second order dispersion × length of the dispersive virtual reference may therefore be described by Eq. (10).

$$D_v(\lambda)L_v = \frac{1}{c}\frac{dN_{gv}(\lambda)L_v}{d\lambda} = \frac{K}{c} \tag{10}$$

In Eqs. (9) and (10), $K$ controls the slope of $N_{gv}(\lambda)L_v$ and therefore the value of the second order dispersion $D_v(\lambda)L_v$. We also observe in Eq. (9) that $b$ and $a$ may be used in conjunction to determine the value of $N_{gv}(\lambda)L_v$ (determined by $b$ when $\lambda = a$). $b$ must be selected such that $N_{gf}(\lambda)L_f$ is balanced by $N_{gv}(\lambda)L_v$ at some wavelength within the available spectral bandwidth, which may be achieved by choosing $a = (\lambda_{\min} + \lambda_{\max})/2$. An estimate for the value of $b$ that balances the test path at $a$ may be found using $b = N_{gv}(a)L_v = N_{g_f}(a)L_f \cong a^2/2T_{avg}(a)$ [9]. The effect of compression, achieved by using a dispersive virtual reference, is visualized by the two interferograms shown in Fig. 2, where a using a dispersive virtual reference with $K < 0$ compresses the interferogram compared to using a non-dispersive reference with $K = 0$.

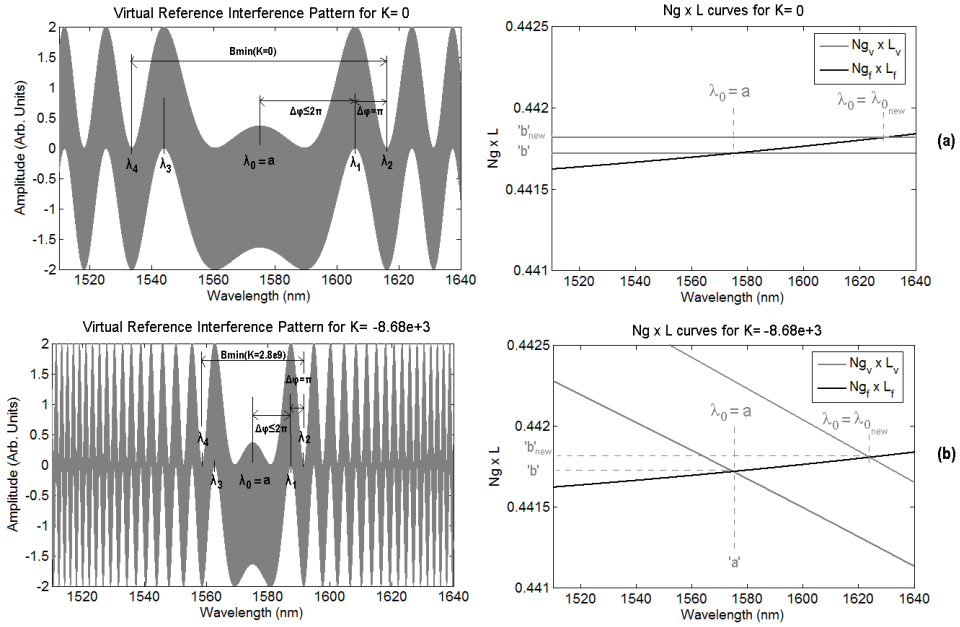


Fig. 2. Plot of the dispersive virtual reference interferograms and group index × length curves for (a) K = 0 (VRI with a non-dispersive reference) and (b) DVRI using K = –8.68e + 3. Two $N_{gv}(\lambda)L_v$ curves are superimposed to show the curves that generate intersections at $\lambda_0 = a$ and $\lambda_0 = \lambda_{0\,\text{new}}$.

#210066 - $15.00 USD Received 14 Apr 2014; revised 23 May 2014; accepted 29 May 2014; published 3 Jun 2014

The group delay plots in Fig. 2 show two superimposed $N_{gv}(\lambda)L_v$ curves to illustrate balancing at $\lambda_0 = a$ (interferogram shown for this case) and $\lambda_0 = \lambda_{0\,\text{new}}$. The balance point $\lambda_0$ in the interferogram corresponds to the intersection point in the group delay plots where $N_{gv}(\lambda_o)L_v = N_{gf}(\lambda_o)L_f$. The two $N_{gv}(\lambda)L_v$ curves illustrate how $\lambda_0$ may be varied by changing the value of $b$ in Eq. (9) to some new value (i.e. $b_{\text{new}}$). Therefore, by sweeping the value of $b$ and tracking $\lambda_0$, the first order dispersion (group delay) of the fiber may be plotted. Note that the difference in the slope of the curves at the intersection point is directly proportional to the magnitude of the compression given by $|\Delta(\lambda_0)|$ and controlled by $D_v(\lambda_0)L_v$ in Eq. (8). The second order dispersion of the fiber may be extracted directly from the interference pattern in Fig. 2 by solving for $|\Delta(\lambda_0)|$ in Eq. (7) using a peak/valley pair (with known phase separation) on each side of $\lambda_0$ (i.e. $\lambda_2$ and $\lambda_1$ as well as $\lambda_4$ and $\lambda_3$) to generate a system of equations using Eq. (7). After solving for $|\Delta(\lambda_0)|$, the second order dispersion may then be extracted by combining Eqs. (8) and (10) given $\text{sgn}(D_v(\lambda_0)L_v) = -\text{sgn}(K)$ (where sgn determines if the sign is positive or negative) and assuming $|D_v(\lambda_0)L_v| > |D_f(\lambda_0)L_f|$, summarized in Eq. (11).

$$D_f(\lambda_0)L_f = \frac{1}{c}\left(K - \text{sgn}(K)|\Delta(\lambda_0)|\lambda_0\right) \tag{11}$$

## 3. Experiments

In this section DVRI experiments are carried out on standard fibers and erbium doped gain fiber. The experimental setups used to generate a real interference pattern in standard fibers and polarization maintaining gain fibers are illustrated in Figs. 3(a) and 3(b), respectively. In both setups the light is launched into the test fiber from an angled facet so that only one reflection is produced at the interface between the launch fiber and the front facet of the test fiber. An interference pattern is then produced using the reflections from the front and end facets of the test fiber. This common path interferometer setup is preferred to using a dual arm interferometer since it does not require calibration of the dispersion of the optical elements used in the (physical) reference path of these interferometer setups. Eliminating the need for calibration also removes the associated calibration error, making this configuration more accurate than a dual arm interferometer.

#210066 - $15.00 USD Received 14 Apr 2014; revised 23 May 2014; accepted 29 May 2014; published 3 Jun 2014

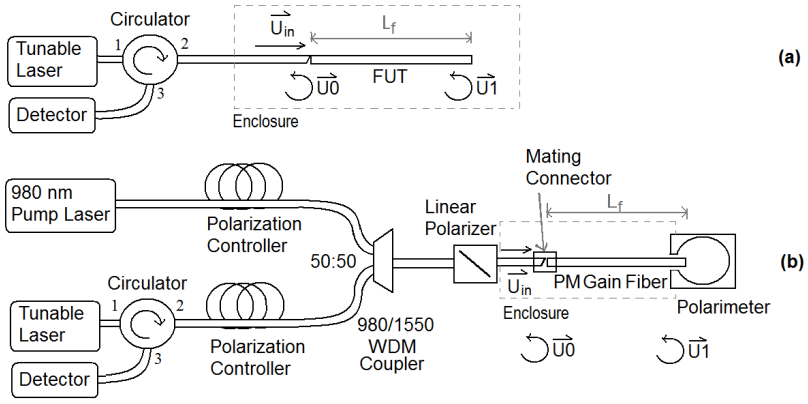


Fig. 3. Setup for dispersion measurement of (a) standard fibers (b) polarization maintaining gain fiber.

A tunable laser (Agilent 81600B Option 160 or 200) is swept continuously over a given bandwidth (experiment dependent) at 10 nm/s and an optical detector connected to a data acquisition card samples the signal at 100 kHz. The laser contains a built-in wavelength meter with a resolution of 0.1 picometers and is capable of automatic wavelength calibration. The interference pattern is plotted as a function of wavelength by synchronizing the timing of wavelength and signal sampling. The tunable laser is connected to port 1 of a fiber optic circulator and a detector is connected to port 3. In order to characterize gain, the setup in Fig. 3(b) is converted to the transmission based gain measurement to enable measurement of gain for each polarization mode in polarization maintaining erbium doped fiber. This is done by replacing the polarimeter in Fig. 3(b) with a 980/1550 nm WDM coupler, and moving the detector from port 3 of the circulator to the 1550 nm side of the WDM coupler. The gain for a given pumping condition is measured by comparing the intensity scan from the test fiber to a background measurement without the gain fiber.

### *3.1 Experimental validation of theory*

In this section DVRI is validated by comparing measurement results on SMF28 fiber to results produced via VRI (previously validated in [9]) and to the manufacturer's specification. The experimental setup for the validation is illustrated in Fig. 3(a). This experiment uses a tunable laser with a wide 200 nm bandwidth (Agilent 81600B Option 200) tuned from 1440 nm to 1640 nm. The wide bandwidth is required for this validation experiment so that VRI may be used to characterize the fiber over a wide wavelength range. After validation, a tunable laser with a smaller bandwidth will be used in the DVRI experiments to illustrate the need for a dispersive reference when bandwidth is limited. The results of the comparison shown in Fig. 4 indicate excellent agreement between both techniques and the manufacturer's specification. The accuracy of the measurements, defined by the standard deviation of the measured group delay and dispersion × length plots, with respect to simulations based on the manufacturer's specification [10], was found to be $2.7 \times 10^{-3}$ ps and $5.2 \times 10^{-5}$ ps/nm, respectively. Note that the maximum deviation from the specification of the group delay and dispersion × length points, within the measurement range was $4.9 \times 10^{-3}$ ps and $8.6 \times 10^{-5}$ ps/nm, respectively. The precision of the group delay measurement, defined as the standard deviation of the measured points with respect to a second order polynomial fit was found to be $9 \times 10^{-4}$ ps. The precision of the dispersion × length measurement, defined as the standard deviation of the measured points with respect to a linear fit was found to be $1.9 \times 10^{-5}$ ps/nm. The dispersion slope (found from a linear fit to the dispersion × length curves) was found to be $4.7 \times 10^{-2}$ ps/nm$^2$·km in both the VRI and DVRI measurement compared to $5.5 \times 10^{-2}$

#210066 - $15.00 USD Received 14 Apr 2014; revised 23 May 2014; accepted 29 May 2014; published 3 Jun 2014

ps/nm$^2$·km in the simulation. The results in Fig. 4 illustrate that the wavelength range over which dispersion measurements may be achieved may also be increased by using DVRI.

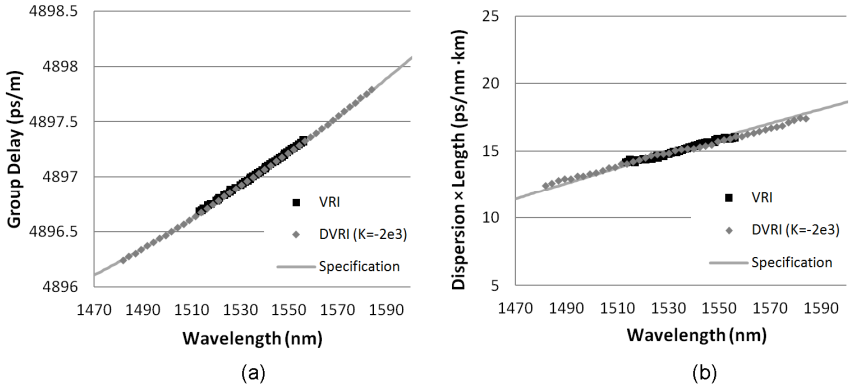


Fig. 4. Measurements of (a) group delay and (b) dispersion parameter on a 20cm length of SMF28 using VRI and DVRI (K = –2e + 3).

### *3.2 Measurement of polarization maintaining erbium doped gain fiber*

In this section DVRI is used to characterize both polarization modes of a 23.3-cm length of polarization maintaining erbium doped gain fiber as a function of pump power using the setup in Fig. 3(b). This fiber has a low second-order dispersion parameter (less than half that of SMF28) and the loss in the unpumped fiber limits the length that may be characterized. As a result, the total *DL* product of the test fiber in this experiment was as low as 0.0012 ps/nm, so that using Eq. (6) this measurement would require over 200 nm, far exceeding the 145 nm bandwidth of the source. This measurement, therefore, would not be possible without using a dispersive reference to compress the interference pattern so that it is within the bandwidth of the source. In the experimental setup shown in Fig. 3(b) the output of a 980 nm pump laser (Lumics LU0980M500) is coupled via a WDM coupler to the output of port 2. Since this gain fiber is birefringent, both signal and pump power must be coupled to one polarization mode at a time using polarization controllers and a linear polarizer at the output of the WDM coupler. The linear polarizer used is broadband with an extinction ratio greater than 20 dB for both 980 nm and 1550 nm light. The polarization controllers are adjusted to maximize the power from the tunable laser and the pump laser at the output of the linear polarizer. The polarization of the light launched into the birefringent gain fiber is controlled by rotating the polarizer at the launch side of the polarization maintaining gain fiber and observed using a polarimeter (PAT 9000) to ensure that light is coupled to one polarization mode at a time. For each polarization mode and pump (gain) setting, the tunable laser (Agilent 81600B Option 160) is tuned from 1495 nm to 1640 nm and the detector samples the signal. Dispersion measurements are then performed from the sampled signal using DVRI. Gain measurements are performed by replacing the polarimeter with a WDM to filter out the pump light and connecting the detector to the signal port of the WDM. The dispersion and gain measurements are then repeated for the other polarization mode. The results of the gain and group delay measurements are illustrated in Figs. 5(a) and 5(b). The standard deviation of the measured group delay curves with respect to a sixth order polynomial fit was found to be on the order of $10^{-3}$ ps for all curves. The results of dispersion parameter measurements obtained by differentiation of the sixth order polynomial fit to the group delay curves, illustrated in Figs. 6(a) and 6(b). In general, it is expected that the first and second order dispersion will change in the gain region since a change in absorption (or gain) is associated with a change in refractive index through the Kramers-Kronig relations. Furthermore, the general shape of the curves in Figs. 5 and 6 are consistent with the curves obtained in [5] for erbium doped fiber.

#210066 - $15.00 USD Received 14 Apr 2014; revised 23 May 2014; accepted 29 May 2014; published 3 Jun 2014

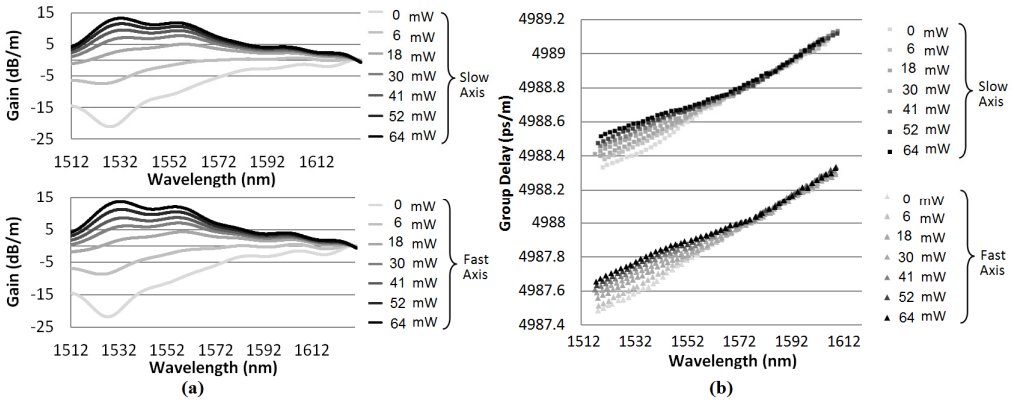


Fig. 5. (a) Gain and (b) group delay curves for a 23.3 cm Erbium doped PM Gain fiber pumped at 980 nm at various pump powers for both fast axis and slow axis measured using DVRI (K = –7.75e + 3).

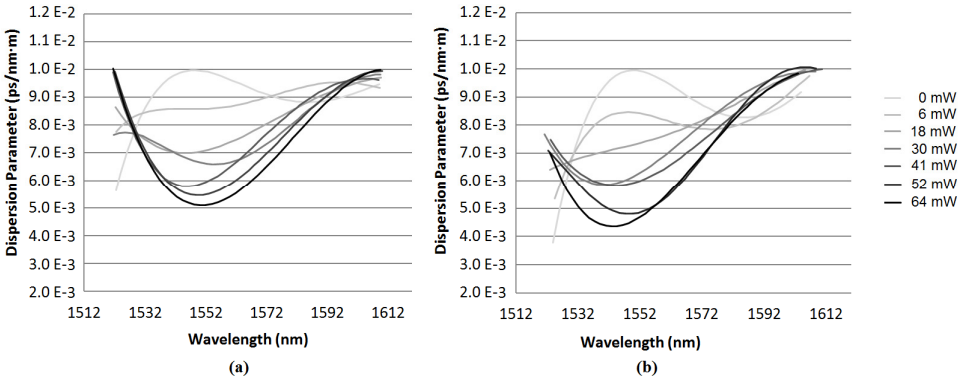


Fig. 6. Dispersion parameter curves for a 23.3 cm length of Erbium doped PM Gain fiber pumped at 980 nm for both (a) fast and (b) slow axes at various pump powers via DVRI (K = –7.75e + 3).

### *3.3 Measurement of dispersion shifted fiber*

In this experiment, the DVRI technique is pushed to the limit to measure a 28.6-cm length of dispersion shifted fiber (DSF) across the zero-dispersion region using a limited bandwidth of 145 nm. The DSF is characterized using the setup illustrated in Fig. 3(a). The tunable laser (Agilent 81600B Option 160) is tuned from 1495 nm to 1640 nm. Measured group delay curves are shown in Fig. 7(a) and dispersion parameter curves found using Eq. (11) are provided in Fig. 7(b). The standard deviation of the measured group delay points with respect to a third order polynomial fit was found to be $1.4 \times 10^{-3}$ ps. The standard deviation of the measured $DL$ points with respect to a linear fit was found to be $4.0 \times 10^{-5}$ ps/nm. The zero-dispersion wavelength and the dispersion slope (slope of the dispersion parameter) are also of interest for DSF. After inversion of the axes in (b) followed by a linear fit, a linear regression analysis gives the zero-dispersion wavelength as 1566.7 nm (consistent with the zero-dispersion wavelength specification provided by the manufacturer) with a precision of ± 0.2 nm and the dispersion slope as $8.57 \times 10^{-5}$ ps/(nm$^2$·m) with a precision ± $0.06 \times 10^{-5}$ ps/(nm$^2$·m). These measurements would not be possible given the bandwidth of this laser if a dispersive reference was not used since $\Delta(\lambda_0) = 0$ in Eq. (6) at the zero-dispersion wavelength.

#210066 - $15.00 USD Received 14 Apr 2014; revised 23 May 2014; accepted 29 May 2014; published 3 Jun 2014

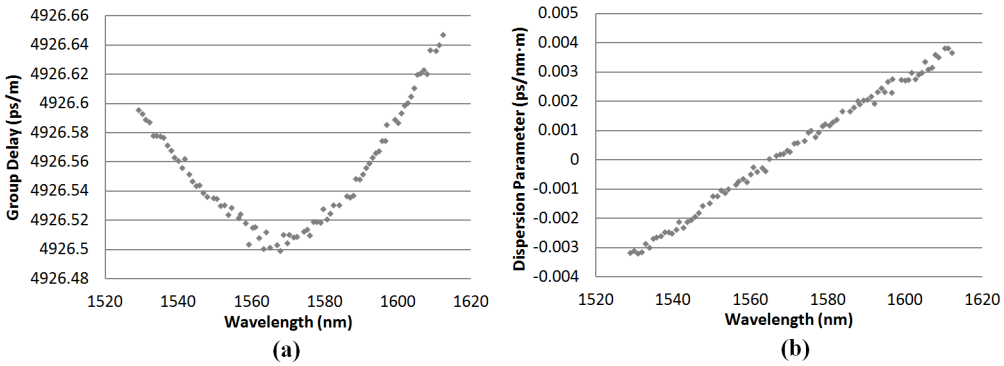


Fig. 7. Measurements of (a) group delay (b) dispersion parameter via direct measurement on dispersion shifted fiber using DVRI (K = −8e + 3).

## 4. Conclusion

This manuscript developed the theory of Dispersive Virtual Reference Interferometry and demonstrated its usefulness for eliminating the *DL* measurement limit for short-length (<1 m) low-dispersion fibers by compressing the interference pattern. It is an important capability when the bandwidth of available sources is limited. Compression of the interferogram has the additional benefit of enabling the generation of dispersion plots over a wider spactral range. The use of a dispersive virtual reference extends the flexibility, versatility and practical utility of the virtual reference technique.

## Acknowledgments

This project is funded by NSERC Discovery, CFI, and ORF Grants. Michael Galle would like to thank the Vanier Canada Graduate Scholarship program for supporting this research.

#210066 - $15.00 USD Received 14 Apr 2014; revised 23 May 2014; accepted 29 May 2014; published 3 Jun 2014